Concentration quenching in an Er-doped phosphate glass for compact optical lasers and amplifiers

Concentration quenching in an Er-doped phosphate glass for compact optical lasers and amplifiers

An additional advantage offered by some glass compositions in terms of device engineering is the possibility to shape the gain medium in the form of fibre or small diameter (below 1 mm) rod. These geometries allow for combining high beam quality, high gain and yet efficient heat extraction along a few centimetres long device [5].

With the aim of developing a compact short pulsed laser as a source for Laser Imaging Detection and Ranging (LIDAR) systems operating at 1.5 μm, Er^{3+}-doped phosphate glass appears as an obvious material candidate for the booster amplifier module.

Phosphate glasses possess several attractive properties with regards to photonics device engineering. They can be processed relatively easily, they show good chemical durability, excellent optical properties, and they offer ion exchangeability [6]. More interestingly, as a host, phosphate glass allows for high RE ions solubility, i.e. clustering effect does not take place or only at very high RE ion concentrations [7]. This latter property makes phosphate glass an interesting alternative to the more traditional and employed silica-based glasses for the development of compact lasers and optical amplifiers [8,9,10,11]. For instance, phosphate glass is particularly interesting when pulsed sources with limited stimulated Brillouin scattering (SBS) are sought, since the high doping level of the phosphate glass hosts can be combined with a large core area single mode configuration [12]. In recent years, these features have made phosphate glass an attractive rare-earth host matrix also in other research fields, like optical communications [8] and microsurgery [13]. As an example, phosphate optical fibres have proven mature for developing reliable 4 kW peak power nanosecond pulsed lasers and single frequency femtosecond pulsed optical amplifiers operating at 1.5 μm [14], both in all-fibre configuration.

It is worth highlighting, however, that even for phosphate glasses a too large amount of RE ions results in concentration quenching caused by ions clustering [15,16]. This non-radiative decay process is detrimental because it leads to a loss of excitation with consequent reduction of fluorescence emission [17]. Within this framework, a careful analysis aimed to estimate the optimal RE doping concentration proves to be essential, considering that erbium concentration quenching in phosphate glass was reported in few papers [18,19,20], since most of the research activity on this subject was dedicated to silica-based glass.

Numerous phosphate laser glass compositions are commercially available from international manufacturers, such as Schott and Kigre [21,22]. However, these latter compositions are not suitable for post-fabrication thermal processing in fibre or small diameter rod forms as crystallization occurs before reaching the suitable process temperature. Additionally, their refractive index is too low for engineering thermally compatible cladding glasses with high refractive index contrast for the fabrication of double cladding fibre structures with efficient pump laser confinement.

This paper reports on the design and development of an Er^{3+}-doped phosphate glass composition meeting the following specifications:

- High glass transition temperature and coefficient of thermal expansion lower than 10^{-6} $°C^{-1}$, for high power handling and thermal shock resistance.

- High thermal stability for optical fibre or small diameter rod manufacturing. A glass stability of at least 200 °C was initially targeted.

- Refractive index of at least 1.56, which allows the possibility for engineering a suitable "low" refractive index phosphate cladding glass with compatible thermo-mechanical properties for the fabrication of a double cladding fibre structure. A numerical aperture (NA) of at least 0.6 between the first and the second cladding was targeted.

- Er^{3+} radiative lifetime of at least 7 ms, in line with the commercially available glasses and with the ones reported in literature.

- High rare earth ion solubility above 10^{21} ions/cm^3 free of clustering. This a requirement for the development of high gain over a short path length laser or amplifier.

2. Materials and methods

2.1 Glass fabrication

Glass samples used in this work were synthesized by conventional melt-quenching method using chemicals (P_2O_5 - Li_2O - Al_2O_3 - BaO - MgO - Gd_2O_3) with high purity level (99+%). The host glass was *ad hoc* developed for this research in view of fabricating a stable and robust glass, able to incorporate high amount of RE ions and suitable for fibre drawing.

Five different glasses, named for short Er1 ÷ Er5, were obtained by doping the host material with an increasing level of Er_2O_3 (ranging from 0.01 to 5.25 mol %) added in substitution of Gd_2O_3. The chemicals were weighted and mixed within a dry box in order to minimize the hydroxyl ions (OH^-) content in the glass.

The batched chemicals were melted at a temperature of 1400 °C for 1 h in a vertical furnace under controlled atmosphere to minimize the content of OH^- groups in the glass.

The melt was cast into a preheated brass mould, then annealed at a temperature around the transition temperature, T_g, for 3 h to relieve glass internal stresses, and finally cooled down slowly to room temperature. The obtained glasses were cut and optically polished to 1 mm-thick samples for optical and spectroscopic characterization.

2.2 Glass characterization

The density of the glasses was measured at room temperature by the Archimedes' method by using distilled water as immersion fluid. The Er^{3+} ion concentrations were calculated from measured sample densities and their initial compositions.

Thermal analysis was performed on fabricated glasses using a Netzsch DTA 404 PC Eos differential thermal analyzer up to 1200 °C with a heat rate of 5 °C/min in sealed Pt/Rh pans. Thermal analysis was carried out in order to measure the characteristic temperatures T_g (glass transition temperature) and T_x (onset crystallization temperature). An error of ± 3 °C was observed in measuring the characteristic temperatures.

The coefficient of thermal expansion (CTE) was measured with a horizontal alumina dilatometer (Netzsch, DIL 402 PC) on 5 mm long specimens operating at 5 °C/min up to 1200 °C. The measure was automatically interrupted when shrinkage higher than 0.13% was reached (softening point). CTE values were calculated in the 200-400 °C temperature range.

The refractive index of the glasses was measured at 1.3 μm, where Er^{3+} ions do not display ground state absorption, by prism coupling technique (Metricon, model 2010). Ten scans were performed for each measurement. Estimated error of the measurement was ± 0.001.

The absorption spectra were measured at room temperature for wavelengths ranging from 350 to 3000 nm using a double beam scanning spectrophotometer (Varian Cary 500).

Fourier transform infrared (FTIR) spectrometer (Alpha, Bruker Optics, Ettlingen, Germany) working in transmission mode and equipped with a DTGS detector was employed. Spectra of the five samples with different Er_2O_3 content were taken between 1800 and 7500 cm^{-1}, with a resolution of 4 cm^{-1} and acquiring an average of 16 scans. OPUS software (v. 6.5, Bruker Optics, Ettlingen, Germany) was used for instrumental control and for spectral acquisition. The transmittance FTIR spectra are reported in terms of attenuation loss.

CW photoluminescence spectra in the near infrared were acquired by a Jobin Yvon iHR320 spectrometer equipped with a Hamamatsu P4631-02 detector, using standard lock-in technique, while in the visible range a photomultiplier Hamamatsu R928P was used. Emission spectra were obtained by exciting the sample with a monochromatic light at the wavelengths of 976 nm, emitted by a single mode fibre pigtailed laser diode (CM962UF76P-10R).

The fluorescence lifetime of Er^{3+}:$^4I_{13/2}$ level was obtained by exciting the samples with light pulses of the 976 nm laser diode, recording the signal by a digital oscilloscope (Tektronix TDS350) and fitting the decay traces by single exponential. Estimated error of the measurement was ± 0.20 ms. The detector used for this measurement was a Thorlabs PDA10CS.

All measurements were performed at room temperature.

2.3 Setup of optimal conditions for glass fabrication

In order to target a good quality optical material for emission in the eye-safe wavelength region, the control of water content in the glass is crucial. To this aim a preliminary work was devoted to the definition of a glass fabrication protocol able to minimize OH^- content in the prepared glasses. For this work a set of glass samples with the same content of Er^{3+} ions (2.6×10^{20} cm^{-3}) was prepared by varying the procedure for mixing the batch chemicals and the glass melting and processing conditions. As control parameters, in particular, the lifetime value of Er^{3+}:$^4I_{13/2}$ level and the absorption of the glass samples at 3000 cm^{-1} were selected. The resulting fabrication procedure was employed for the fabrication of the Er1 ÷ Er5 glasses studied in this paper.

3. Results and discussion

3.1. Definition of the procedure for glass fabrication

The preliminary work aiming at defining the glass fabrication protocol allowed assessing a precise correlation between the Er^{3+}:$^4I_{13/2}$ level lifetime and the glass water content. Twelve glass samples were fabricated for this study and Fig. 1 shows the results of the measurement campaign, which demonstrate that a careful control of the overall fabrication process is crucial in achieving high quality glasses. The main improvements regarded the selection of high purity chemicals, the use of a dry box to weigh the chemicals and the flow of dry air inside the furnace during glass melting.

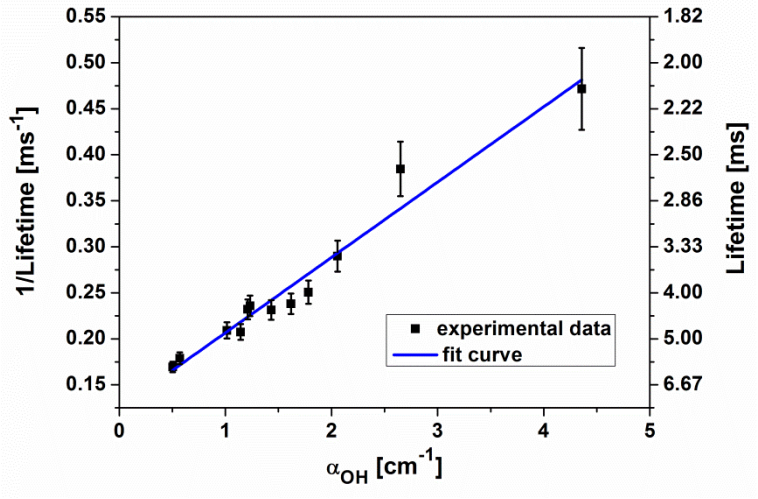

Fig. 1. Decay rate, defined as the inverse of the Er^{3+}:$^4I_{13/2}$ level lifetime, as a function of the absorption coefficient α_{OH} of OH^- vibration band at 3000 cm^{-1} of all glass samples prepared for the definition of the optimized fabrication process. The experimental data were fitted through the formula (2) reported in Ref. [23]. For the benefit of the reader, measured lifetime values are reported on the right y-axis.

3.2. Glass physical and thermal properties

All fabricated glasses were crystallization free and homogeneous.

Table 1 reports their thermal properties, density, refractive index and the calculated Er^{3+} ions concentration.

It is worth noting that the physical properties did not change significantly by varying the doping level of the glasses, due to the fact that the doping oxide Er_2O_3 was added in substitution of Gd_2O_3 in the host matrix, both quite close in terms of molecular weight.

An average value of ΔT = 496 ± 3 °C was measured, which suggests that these glasses are very stable against de-vitrification and suitable for crystal-free fibre drawing. Furthermore, a typical linear thermal expansion coefficient value of 9×10^{-6} $°C^{-1}$ was assessed, which is similar to other phosphate glasses [24], but an order of magnitude higher than silica glasses.

It is worth highlighting that these glasses show T_g and CTE values respectively higher and slightly lower than those of APG-1 phosphate laser glass for high power applications manufactured by Schott [21], thus illustrating their potential for high power handling and high thermal shock resistance.

Table 1

Er^{3+} ions content in mol%, Er^{3+} ions concentration, glass transition temperature (T_g), crystallization temperature (T_x), density, and refractive index of the manufactured phosphate glasses.

Glass label	**Er^{3+} [mol%]**	**Er^{3+} [$\times 10^{20}$ ions/cm^3]**	**T_g [°C] ± 3 °C**	**T_x [°C] ± 3 °C**	**$\Delta T=T_x-T_g$ [°C] ± 6 °C**	**ρ [g/cm^3] ± 0.05 g/cm^3**	**n ± 0.001**
Er1	0.02	0.02	485	1017	532	3.42	1.570
Er2	1	1.30	489	986	497	3.45	1.573
Er3	2	2.59	482	1009	527	3.41	1.569
Er4	6	7.76	480	889	409	3.42	1.568
Er5	10	13.73	495	1008	513	3.47	1.570

3.3. Absorption and transmission spectra

UV-Vis and FTIR analyses were carried out on all prepared samples and absorption and transmission spectra were respectively recorded.

Absorption cross-section σ_a [cm^{-3}] was calculated from experimental data using the following formula:

$$\sigma_a(\lambda) = \frac{2.303 \log\left(\frac{I_0}{I}\right)}{NL}$$

where $log(I_0/I)$ is the absorbance, L the glass sample thickness in cm and N is the concentration of the Er^{3+} ions per cm^3.

Fig. 2 shows the absorption cross-section values obtained for glass sample Er5. The inhomogeneously broadened bands are assigned to the transitions from the ground state $^4I_{15/2}$ to the excited states of Er^{3+} ions (see inset of Fig. 2).

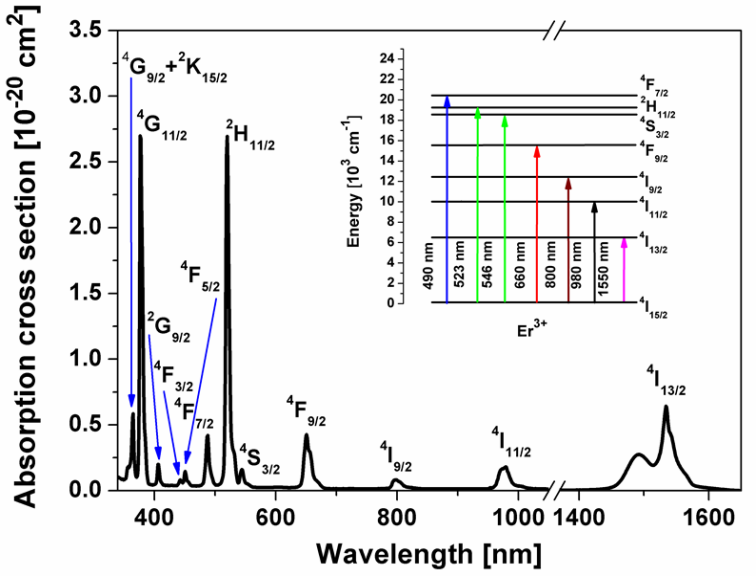

Fig. 2. Absorption cross-section spectrum of sample Er5. The main Er^{3+} levels are labeled, considering absorption from the ground state $^4I_{15/2}$. The inset shows the Er^{3+} ion energy levels.

Fig. 3 shows the IR spectrum of glass sample Er5 between 1800 and 7500 cm^{-1}, as an example. In the medium IR region, between 1800 and 4000 cm^{-1}, the spectrum clearly reveals a group of prominent absorption bands due to the hydroxyl groups and very weak peaks at around 2850 cm^{-1} due to some organic contaminants on the surface of the samples. In the NIR region a broad and intense band associated with the transition from the ground state $^4I_{15/2}$ to the excited level $^4I_{13/2}$ of the Er^{3+} ions is detected at around 6500 cm^{-1}.

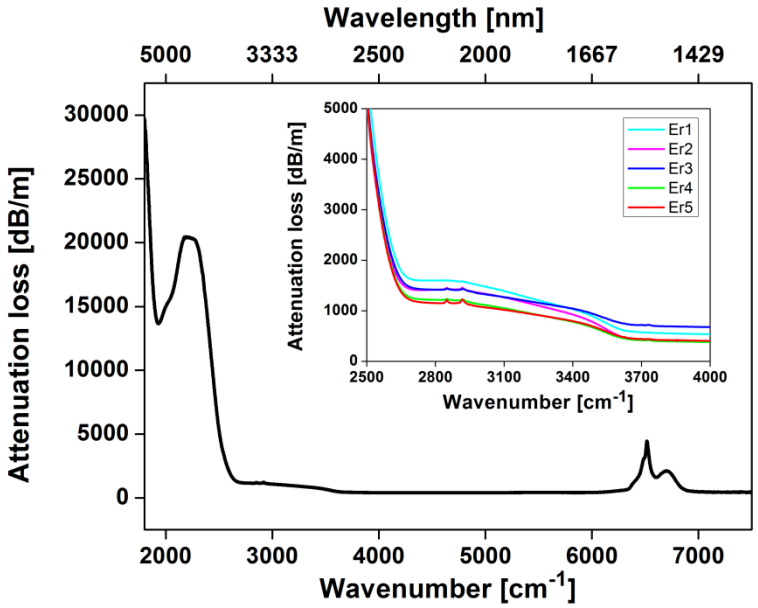

Fig. 3. IR spectrum of glass sample Er5; the inset shows the zoom-up of the OH^- broad band at 3000 cm^{-1} of all the manufactured samples Er1 ÷ Er5.

Phosphate glass hosts are well known from the literature to be particularly vulnerable to OH^- contamination because they tend to absorb water molecules readily during melting process, and although sophisticated methods may be used, some residual hydroxyl groups remain in the glass typically at concentrations greater than 100 ppm, even in commercial phosphate laser glasses [25].

As it can be clearly noticed in Fig. 3, the main contribution due to the presence of water in the glass host is given by the intense peak observed at about 2200 cm^{-1} [26]. Nevertheless, a greater interest is commonly devoted to the broad band at about 3000 cm^{-1}, since it provides useful information on the concentration of OH^- groups inside the glass. The content of hydroxyl groups has been evaluated through the application of the formulas proposed by Speghini *et al.* [27] and Ehrmann *et al.* [25], and medium values of 21 and 170 ppm have been respectively obtained.

The inset of Fig. 3 reports the zoom-up of the spectra of the five samples with different erbium content (Er1 ÷ Er5) in the region between 2500 and 4000 cm^{-1}. It is worthwhile noting that in this medium IR region the spectra show a similar profile for all glasses, thus demonstrating that the manufacturing process has been correctly optimized and standardized.

3.4. Infrared and up-conversion luminescence spectra

Normalized fluorescence spectra of the Er^{3+}-doped glass samples, measured in the wavelength range 1400 ÷ 1700 nm under excitation at 976 nm, are illustrated in Fig. 4. A broad and intense emission is evident, which is assigned to the Er^{3+}:$^4I_{13/2} \rightarrow {}^4I_{15/2}$ transition.

The FWHM is a critical parameter commonly used to evaluate the gain bandwidth properties of the optical amplifiers. In the manufactured samples, it slightly increases with increasing the Er^{3+} concentration. Values range from 30 to 39 ± 2 nm, similar to other phosphate glasses (37 nm) and to silicate glasses (40 nm) [28].

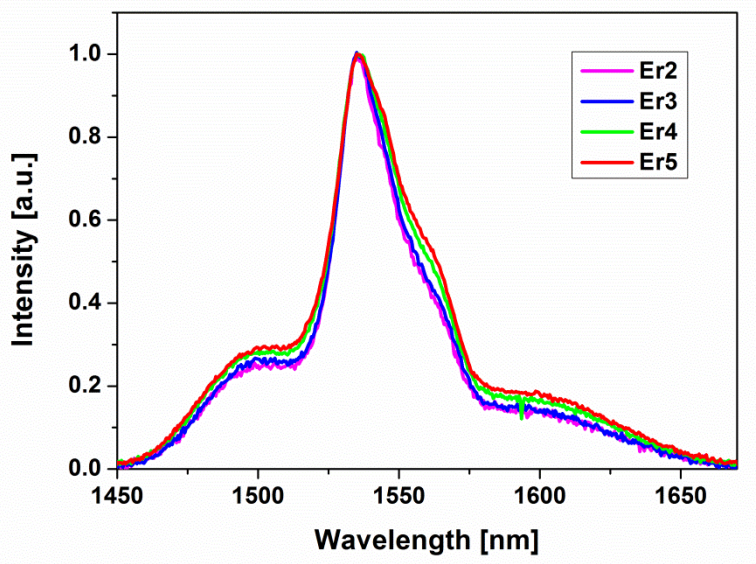

Fig. 4. NIR emission spectra of the manufactured phosphate glass samples obtained under excitation at 976 nm with a CW laser diode. Er1 spectrum is not reported since it displays a poor signal to noise ratio.

During measurement, a visible green emission arising from the glass samples was noticeable to the naked eyes. The green luminescence was showed to increase with increasing pump power. Fig. 5 reports the fluorescence spectra of the Er^{3+}-doped glass samples, in the wavelength range 500 ÷ 850 nm, under excitation at 976 nm. Visible emission of sample Er1 was too low to be measured.

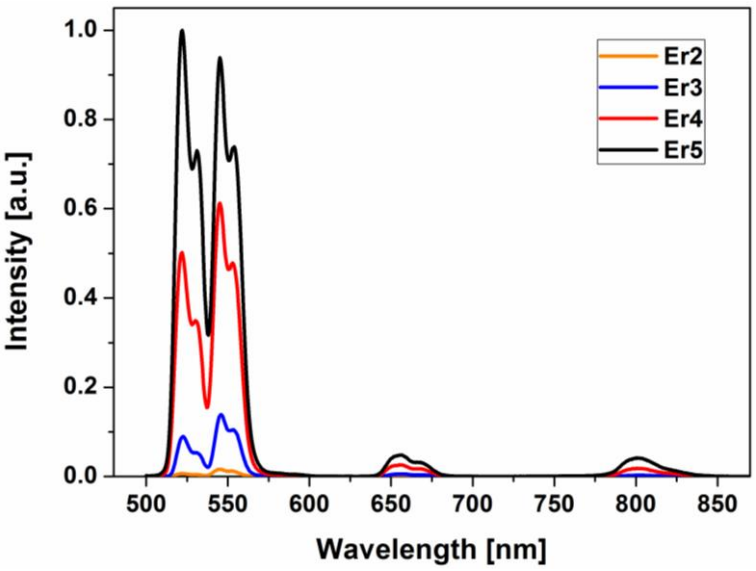

Fig. 5. Emission spectra of the manufactured phosphate glass samples in the wavelength range 500 ÷ 850 nm obtained under excitation at 976 nm with a CW laser diode. The intensities of the emission are normalized to the green up-conversion band (523 nm) of sample Er5. Visible emission of sample Er1 was too low to be measured.

Although the luminescence appears green to the naked eye, the measurement showed some amount of red contents. Green peaks barycenter wavelengths (523 nm and 546 nm) match the corresponding emission

wavelengths of the Er^{3+} energy levels $^2H_{11/2}$ and $^4S_{3/2}$, while the red peak (655 nm) is in agreement with the $^4F_{9/2}$ one. Emission centered at 800 nm originates from the transition $^4I_{9/2} \rightarrow {}^4I_{15/2}$ [29].

Population of these upper excitation levels is due to concentration quenching of Er^{3+} ions in glass that is believed to be dominated by cooperative up-conversion processes [15]. In fact 980 nm pump radiation does not suffer from excited state absorption (ESA) from the metastable $^4I_{13/2}$ level [15,30].

3.5. Fluorescence lifetime

For optical amplifiers or lasers operating at 1.55 μm, an important parameter is the Er^{3+}:$^4I_{13/2}$ level lifetime: the longer the lifetime, the higher the population inversion between this level and the ground state.

Examples of the luminescence decay curves of the $^4I_{13/2} \rightarrow {}^4I_{15/2}$ emission upon 976 nm excitation are reported in Fig. 6, while the corresponding lifetime values, calculated for all glass samples, are listed in

Table 2 and reported as a function of the Er^{3+} ion concentration in Fig. 7.

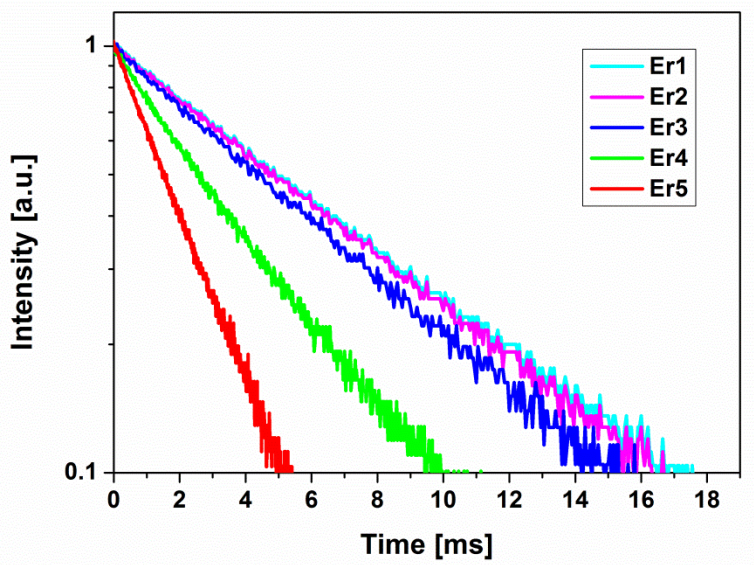

Fig. 6. Room temperature decay curves of the $^4I_{13/2}$ level of Er^{3+} ions in the manufactured samples obtained under excitation at 976 nm. The intensity data are reported on a Log scale.

Table 2

Excited state $^4I_{13/2}$ lifetime values for Er^{3+} doped samples under laser excitation at 976 nm.

Glass label	**Er^{3+} [mol%]**	**Er^{3+}:$^4I_{13/2}$ lifetime [ms] ± 0.20 ms**
Er1	0.02	7.04
Er2	1	7.01
Er3	2	6.33
Er4	6	3.60
Er5	10	2.11

The $^4I_{13/2}$ lifetime trend is similar to that observed in other phosphate glasses [19,24,31]: lifetime decreases with rising Er^{3+} concentration due to the increase of energy transfer between neighbourhood Er^{3+} ions and energy transfer from Er^{3+} ions to quenching centres like OH^- groups [17,32]. Specially, the free OH^- groups in the glass are regarded as effective quenchers of the IR radiation in Er^{3+}-doped phosphate glasses [33].

The fluorescence lifetime experimental data were fitted by the empirical formula proposed by Auzel *et al.* [34,35] for the case of limited diffusion, in which the energy transfer from Er^{3+} to nearby defects or trapping centres, also known as quenching traps, is assumed to be the main mechanism responsible for the increase in the quenching process:

$$\tau(N) = \frac{\tau_0}{1 + \frac{9}{2\pi}\left(\frac{N}{N_0}\right)^2}$$

where τ is the measured lifetime at a given Er^{3+} ions concentration (N), τ_0 is the lifetime in the limit of "zero" concentration, i.e. the radiative lifetime, and N_0 is the quenching concentration.

A good agreement (R = 0.9937) with the fit curve for the whole range of concentrations was found (see Fig. 7), and in addition the values of τ_0 = 7.05 ms and $N_0 = 9.92 \times 10^{20}$ ions/cm^3 obtained from the fitting are considerably higher with respect to those reported in literature for other phosphate glasses (τ_0 = 1.09 ms and $N_0 = 2.5 \times 10^{20}$ ions/cm^3 in [28]). The reason is probably due to a reduced incorporation of OH^- groups in our glasses, thanks to the use of controlled dry atmosphere during the melting process. Nonetheless, it is important to mention that the measured lifetime values of our samples remained slightly lower than those shown by commercially available phosphate glasses, which typically exceed 7.5 ms [21,22]. At this stage we believe that the main cause accounting for this difference may reside either in the glass structure itself and in the contamination by other chemical species in addition to OH^- groups such as transition metal ions. Nevertheless, we expect that a lifetime value of 7 ms provides prospect for the development of efficient fibre laser sources and paves the way towards an optical cavity characterized by high efficiency (high lifetime values) and compactness (high concentration of rare earth ions).

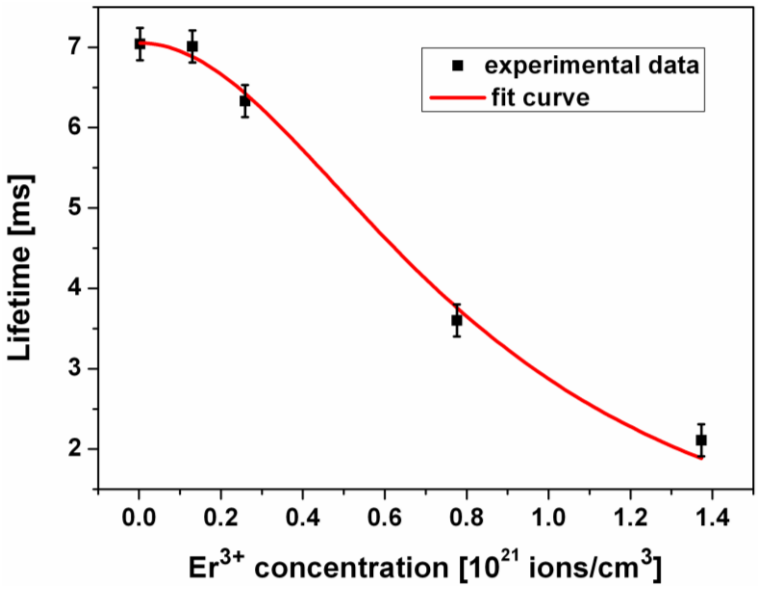

Fig. 7. Experimental and fitted values of Er^{3+}:$^4I_{13/2}$ excited state lifetime in samples Er1 ÷ Er5.

4. Conclusions

This paper reports on the fabrication and the thermal and spectroscopic characterization of five phosphate glasses doped with a variable Er^{3+} ions content. All prepared samples were homogeneous and presented a good thermal stability and thus are suitable for fibre drawing.

The influence of Er^{3+} ions doping concentration on optical properties was investigated in order to study the concentration quenching effect on luminescence performance. With increasing the concentration of Er^{3+} ions, the 1.5 μm emission band became broader, while the lifetime of the $^4I_{13/2}$ state decreased due to unwanted energy transfer between RE ions. FWHM ranged from 30 to 39 ± 2 nm at concentrations of Er^{3+} ions corresponding to 0.02 and 13.73×10^{20} ions/cm^3, respectively.

The fluorescence lifetime data were fitted to the limited diffusion model proposed by Auzel and a radiative lifetime and a quenching concentration of τ_0 = 7.05 ms and N_0 = 9.92×10^{20} ions/cm^3 were respectively obtained.

The next step in this research will be the employment of the studied phosphate glass doped with the optimal erbium concentration for the design and development of a compact and efficient pulsed eye-safe fibre laser source for environmental monitoring and sensing applications. An Er^{3+} ions concentration of around 2.50×10^{20} ions/cm^3, thus similar to Er3, represents a good trade-off between the request of a high doping level for compactness and a high lifetime of the Er^{3+}:$^4I_{13/2}$ emitting level for an efficient operation.

Acknowledgements

The authors acknowledge the COST Action MP1401 “Advanced Fibre Laser and Coherent Source as tools for Society, Manufacturing and Lifescience” for the support of this research effort.

References

[1] M.D. Shirk, P.A. Molian, J. Laser Appl. 10 (1998) 18.

[2] A.R. Nassar, E.W. Reutzel, Metall. Mater. Trans. A 46 (2015) 2781–2789.

[3] S. Sato, M. Ogura, M. Ishihara, S. Kawauchi, T. Arai, T. Matsui, A. Kurita, M. Obara, M. Kikuchi, H. Ashida, Lasers Surg. Med. 29 (2001) 464–473.

[4] W. Shi, E.B. Petersen, Z. Yao, D.T. Nguyen, J. Zong, M.A. Stephen, A. Chavez-Pirson, N. Peyghambarian, Opt. Lett. 35 (2010) 2418–2420.

[5] D.J. Richardson, J. Nilsson, W.A. Clarkson, J. Opt. Soc. Am. B 27 (2010) B63-B92.

[6] M. Yamane, Y. Asahara, Glasses for Photonics, Cambridge University Press, Cambridge, 2000.

[7] N.G. Boetti, G.C. Scarpignato, J. Lousteau, D. Pugliese, L. Bastard, J.-E. Broquin, D. Milanese, J. Opt. 17 (2015) 065705.

[8] S. Jiang, T. Luo, B.-C. Hwang, F. Smektala, K. Seneschal, J. Lucas, N. Peyghambarian, J. Non-Cryst. Solids 263&264 (2000) 364–368.

[9] P. Laporta, S. Taccheo, S. Longhi, O. Svelto, C. Svelto, Opt. Mater. 11 (1999) 269–288.

[10] D.L. Veasey, D.S. Funk, P.M. Peters, N.A. Sanford, G.E. Obarski, N. Fontaine, M. Young, A.P. Paskin, W. Liu, S.N. Houde-Walter, J.S. Hayden, J. Non-Cryst. Solids 263&264 (2000) 369–388.

[11] E. Mura, J. Lousteau, D. Milanese, S. Abrate, V.M. Sglavo, J. Non-Cryst. Solids 362 (2013) 147–151.

[12] W. Shi, E.B. Petersen, Z. Yao, D.T. Nguyen, J. Zong, M.A. Stephen, A. Chavez-Pirson, N. Peyghambarian, Opt. Lett. 35 (2010) 2418–2420.

[13] J.C. Knowles, J. Mater. Chem. 13 (2003) 2395–2401.

[14] www.NPPhotonics.com.

[15] W.J. Miniscalco, J. Lightwave Technol. 9 (1991) 234–250.

[16] R. Quimby, W.J. Miniscalco, B. Thompson, J. Appl. Phys. 76 (1994) 4472–4478.

[17] Y. Yan, A.J. Faber, H. de Waal, J. Non-Cryst. Solids 181 (1995) 283–290.

[18] B.-C. Hwang, S. Jiang, T. Luo, J. Watson, G. Sorbello, N. Peyghambarian, J. Opt. Soc. Am. B 17 (2000) 833–839.

[19] T. Ohtsuki, S. Honkanen, S.I. Najafi, N. Peyghambarian, J. Opt. Soc. Am. B 14 (1997) 1838–1845.

[20] C. Jiang, W. Hu, Q. Zeng, IEEE J. Quantum Electron. 39 (2003) 1266–1271.

[21] www.schott.com.

[22] www.kigre.com.

[23] H. Ebendorff-Heidepriem, W. Seeber, D. Ehrt, J. Non-Cryst. Solids 183 (1995) 191–200.

[24] N.G. Boetti, D. Negro, J. Lousteau, F.S. Freyria, B. Bonelli, S. Abrate, D. Milanese, J. Non-Cryst. Solids 377 (2013) 100–104.

[25] P.R. Ehrmann, K Carlson, J.H. Campbell, C.A. Click, R.K. Brown, J. Non-Cryst. Solids 349 (2004) 105–114.

[26] R. Lal, N.D. Sharma, H.K. Sharma, K. Chandra, Indian J. Pure Appl. Phys. 42 (2004) 25–30.

[27] A. Speghini, R. Francini, A. Martinez, M. Tavernese, M. Bettinelli, Spectrochim. Acta, Part A 57 (2001) 2001–2008.

[28] F. Rivera-López, P. Babu, L. Jyothi, U.R. Rodríguez-Mendoza, I.R. Martín, C.K. Jayasankar, V. Lavín, Opt. Mater. 34 (2012) 1235–1240.

[29] M.J.F. Digonnet, Rare-Earth-Doped Fiber Lasers and Amplifiers, Marcel Dekker, Inc., New York, 2001.

[30] R. Francini, F. Giovenale, U.M. Grassano, P. Laporta, S. Taccheo, Opt. Mater. 13 (2000) 417–425.

[31] A.A. Reddy, S.S. Babu, K. Pradeesh, C.J. Otton, G.V. Prakash, J. Alloys Compd. 509 (2011) 4047–4052.

[32] H. Desirena, E. De la Rosa, L.A. Díaz-Torres, G.A. Kumar, Opt. Mater. 28 (2006) 560–568.

[33] X. Feng, S. Tanabe, T. Hanada, J. Non-Cryst. Solids 281 (2001) 48–54.

[34] F. Auzel, F. Bonfigli, S. Gagliari, G. Baldacchini, J. Lumin. 94&95 (2001) 293–297.

[35] F. Auzel, G. Baldacchini, L. Laversenne, G. Boulon, Opt. Mater. 24 (2003) 103–109.